



TECHNICAL UNIVERSITY OF CLUJ-NAPOCA

ACTA TECHNICA NAPOCENSIS

Series: Applied Mathematics, Mechanics, and Engineering  
Vol. 67, Issue I, March, 2024

## COMPARISON OF BEVEL GEARS WITH DIFFERENT PRESSURE ANGLE

Pinar DEMIRCIOGLU, Ismail BOGREKCI, Yegane Mediha MUTLU

**Abstract:** *In the domain of gear mechanisms, clutch engagement initiates precisely at the moment when the lateral side of the rotating tongue makes contact with the apex of the tooth on the rotated gear. Subsequently, clutch disengagement occurs when the uppermost point of the tooth on the rotating gear meets the lateral surface of the rotated gear. Notably, a decrease in the pressure angle corresponds to an increase in the clutch ratio, albeit with an increase in the minimum number of teeth. In this investigation, three sets of gears with pressure angles of  $14.5^\circ$ ,  $20^\circ$ , and  $25^\circ$  were meticulously crafted using KISSsoft for a fertilizer spreader with an input power of 7.5 kW and an input speed of 540 1/min. The study revealed that the gear with a  $25^\circ$  pressure angle performed most effectively for the specified gearbox. These findings underscore the intricate relationship between pressure angle, clutch ratio, and the minimum number of teeth, offering valuable insights into optimal design parameters for enhancing gear system efficiency, as exemplified in the context of a fertilizer spreader application.*

**Key words:** *Bevel gear, gear design software, gear macrogeometry, tooth profile, sliding friction, KISSsoft simulation, pressure angle optimization, specific sliding analysis*

### 1. INTRODUCTION

Throughout history, gear wheels have undergone continuous refinement, evolving from ancient times to the present day. As integral components in power and motion transmission, they serve a crucial role in various applications requiring efficient motion and power transmission systems across industries such as automotive, aerospace, and defense. Among a machine's critical elements, its mobility and powertrain stand out, highlighting the importance of ensuring the consistent, quiet, and effective operation of gear wheels. To achieve this, ongoing research and studies focus on gear wheel optimization, aiming to further enhance their performance. The following provides a summary of relevant studies discussed in the literature.

The paper aimed to establish the optimum specifications for a step gear pair. The focus was on optimizing the gear group within a tractor transmission through a systematic investigation. The design stages of the gearbox were outlined using an optimization flow chart to guide the

process. Notably, the study revealed that surface pressure positively impacts the factor of safety. Additionally, an increase in module was found to positively influence the factor of safety regarding bending stress. However, it was observed that an increase in module had a negative effect on the factor of safety related to surface pressure [1].

The paper explores the dynamic behavior of torsion, bending, and axial forces. It employs a dynamic model that considers multi-state meshing features to comprehensively investigate the system's dynamic properties.

The model scrutinizes dynamic properties via three Poincaré sections and investigates tooth disengagement and backside contact mechanisms by utilizing a time history diagram of the total normal force. Nonlinear dynamics equations are resolved employing the variable step fourth-order Runge-Kutta method. The study finds that impacts primarily arise from tooth separation, with stable drive-side meshing to prevent disengagement impacts, while backside impact occurs at specific tooth disengagement amplitudes [2].

The paper investigates how gear vibration and noise relate to geometric parameters during transmission. Using KISSsoft software, it analyzes how profile modification affects noise levels in a reference gear pair. Graphical findings show that applying the Tip Relief method significantly reduces noise. The study explores the link between geometric changes and noise, illustrating effects through graphs linked with the contact ratio. Higher contact ratios, indicating fewer transmission errors, lead to quieter operation. Additionally, noise increases with lower gear quality and wider gears exacerbate manufacturing errors, resulting in louder operation. These insights shed light on the interplay between geometric parameters and noise in gear transmission [3].

The study introduces a method to enhance the surface contact and bending strengths of gear teeth, utilizing the AGMA GRS 3.1.7 gear rating suite for calculations. To streamline data presentation, a concise approach is adopted. Additionally, it suggests conducting alternative FEA on gear teeth to validate stresses and compare results. Dolan and Broghamer's research on stress reduction parameters is discussed. The methodology involves using top land, contact ratio, and backlash to determine gear tooth pressure angle, but it does not explicitly consider hob tip radius. To address this, a second example is provided with a predetermined hob tip radius. Equations and calculations are adjusted to find the pressure angle corresponding to this radius, concluding it to be smaller and preferable for design compared to scenarios without considering hob tip radius [4].

The study discusses the results of a three-dimensional stress analysis conducted on spur and bevel gears. While Lewis' equation is commonly used for bending stress calculation, it has limitations in considering axial and radial loads. To address this, FEM is employed for robust stress analysis, particularly for bevel gear teeth, an area lacking prior research. The analysis demonstrates the application of cyclic symmetry to spur gears, leading to significant computational savings. This method, incorporating geometrical periodicity and submatrices elimination, can extend to dynamic analyses of gear teeth, offering valuable

advancements in accuracy and efficiency for complex gear systems [5].

The paper presents a combined theoretical calculation and FEM analysis investigating the impact of gear speed on contact stress. The study, conducted at 2.5 kW power, explores fatigue behavior over 108 cycles at speeds of 1200, 1500, and 1800 rpm, considering factors like elasticity coefficient, overload, dynamic load, size, load distribution, and surface condition. Findings reveal a decrease in contact stress with increasing rotational speed, with theoretical calculations and FEM analysis showing consistent results. Utilizing the ANSYS finite element program allows for modeling and observing stress distributions, providing insights into gear structural behavior across various operational conditions [6].

The study introduces an advanced approach to modeling the nonlinear oil film strength of Finite Length Squeeze Film Dampers (FLSFD) in bevel gear systems. It addresses limitations in existing models and proposes a more precise and adaptable model. Comparisons are made between bevel gear systems with and without FLSFD, focusing on damping characteristics. The analysis includes sensitivity to parameters such as FLSFD length and radial clearance. Results show FLSFD effectively reduces vibration amplitudes over critical speeds and establishes correlations between damping performance and FLSFD design parameters, offering insights for optimizing bevel gear system dynamics [7].

The study explores the elastic deformation of gear pairs and employs an orthogonal design approach to identify optimal isometric modification parameters. Subsequently, each tooth is individually modified using these parameters alongside symmetric crowned modification parameters. SolidWorks generates three-dimensional solid models of conventional and modified gears, while ANSYS/LS-DYNA conducts dynamic contact Finite Element Analysis (FEA). Simulation results reveal that ideal isometric modification significantly reduces meshing impact, mitigates "end contact," and more uniformly distributes tooth loads compared to symmetric crowned modification for straight bevel gears. These findings refine the theory of isometric

modification for straight bevel gears, providing valuable insights to enhance gear performance and durability [8].

The study introduces a computerized design approach for precision-forged advanced straight and skew bevel gears. Its aim is to improve gear set performance by optimizing tooth surfaces to localize bearing contact and preemptively address transmission issues. The proposed tooth surface modifications, derived from a modified crown gear model, are intended for implementation during production with appropriately designed dies. The theoretical geometry of each die, crucial for component production, is determined based on the corresponding hypothetical crown gear. Two surface modification approaches, whole and partial crowning, are investigated to identify the most effective method for both skew and straight bevel gears. Additionally, a pre-designed functional solution for transmission faults is included to mitigate gear drive noise and vibration. Numerical examples demonstrating the design of both skew and straight bevel gear drives emphasize the effectiveness of the proposed modifications in enhancing performance and reliability [9].

The study introduces a new method for designing and analyzing formate-generated spiral bevel gears. It aims to achieve stable, low-noise bearing contact while addressing challenges related to formate formation. The method involves four sequential procedures: establishing bearing contact with reduced contact shift due to misalignment, pre-designing a parabolic function of transmission errors, and stress analysis using the finite element method. The developed Finite Element Analysis (FEA) process automatically generates models with multiple pairs of teeth, analyzed using ABAQUS. The approach is validated through computerized simulation and finite element analysis, confirming its effectiveness [10].

The paper proposes using an asymmetric basic rack profile to notably enhance the load capacity of bevel gears. This decision necessitates careful consideration of factors such as the length of the contact line and the shape of the tooth root fillet to achieve the desired performance enhancement. These factors are

crucial in determining the overall effectiveness of the asymmetric basic rack profile in improving the load capacity of bevel gears [11].

This study explores gear macrogeometry across three pressure angles, employing sliding graphs to evaluate mesh efficiency and power losses within gear pairs. Additionally, it computes normal and radial forces on the gears, shedding light on mechanical behavior and performance attributes associated with different pressure angles.

## 2. DESIGN OF GEAR

### 2.1 Input Datas

The table displays input data for three gears, each characterized by distinct pressure angles and profile shift factors. These variations determine the specific specifications for each gear examined in the study.

Table 1

Table of Inputs

Inputs / Gears	Gear Pair 1	Gear Pair 2	Gear Pair 3
Power (kW)	7.5	7.5	7.5
Speed (1/min)	540	540	540
Application Factor	1.25	1.25	1.25
Mean Normal Module	4.043	4.043	4.043
Number of Teeth	15	15	15
Facewidth (mm)	14.5	14.5	14.5
Materials	16MnCr5	16MnCr5	16MnCr5
Profile Shift Coefficient	0.4351/-0.4351	0	0
Lubrication	ISO/VG 150	ISO/VG 150	ISO/VG 150

#### 2.1.1 Application Factor and Mounting Factor

The application factor, standardized at 1.0 as KA, helps to account for uncertainties from loads and impacts. Table 2 outlines the coefficient values according to ISO 10300 standards. Consistent operational behavior is maintained, with the system designed to accommodate moderate shocks.

*Table 2*  
**Linking Application Factors to Operational Behavior**

Operational behavior of the driving machine	Operational behavior of the driven machine			
	uniform	moderate shocks	average shocks	heavy shocks
uniform	1.00	1.25	1.50	1.75
light shocks	1.10	1.35	1.60	1.85
moderate shocks	1.25	1.50	1.75	2.00
heavy shocks	1.50	1.75	2.00	2.25

The "straddle design" involves a shaft extending from both sides of a gear's toothed face, distributing load among shaft-mounted bearings in high-load gear trains. Integrating gear and shaft into a single component presents challenges like potential interference during tooth formation [12]. Mounting conditions adhere to DIN 3991 standard, outlined in Table 3 for reference in various settings.

*Table 3*  
**Mounting factor according to DIN 3991**

Application	Mounting conditions of pinion and gear		
	Both members	One member	Neither member
Aircraft	1.00	1.10	1.25
Automotive	1.00	1.10	1.25
Industry, ship	1.10	1.25	1.50

**2.1.3 Speed, Torque, and Service Life Assessment**

The gears are crafted for their application in the field of fertilizer spreading, where precise control is paramount to ensure the accurate and uniform distribution of fertilizer onto the soil. This process is essential for promoting healthy crop growth by guaranteeing the correct and equitable dispersion of essential nutrients. To

ensure integration with existing machinery, the transmission input speed for these gears is set at 540 rpm, a standard speed commonly found in fertilizer spreaders. This deliberate choice aligns the gears with industry norms, facilitating compatibility and ease of integration. Moreover, the desired service life for the gears is set at 20,000 hours, following the recommendations of KISSsoft software, which identifies this duration as the maximum operational life. This benchmark underscores the commitment to durability and reliability in the design of these gears. Additionally, the input torque for the gearbox, featuring a 1:1 transmission ratio, is carefully determined based on the torque specifications of existing gearboxes in fertilizer spreaders. This consideration ensures that the designed gears not only meet but exceed the operational requirements and torque considerations necessary for optimal performance in the demanding environment of fertilizer spreading machinery.

**2.1.4 Profile Shift Coefficient**

Profile shifting is a technique used to create gears with tooth thicknesses different from those of standard gears. It can impact both the center distance of a gear pair and gear strength. The study investigates addendum modification, known as profile shift, in gears. Increasing addendum thickness enhances bending resistance and reduces contact stress, while decreasing thickness increases bending stress. The profile shift coefficient quantifies this adjustment relative to the module. Factors chosen from KISSsoft's recommendations, depicted in Figures 1-3, play a crucial role in optimizing gear performance by influencing bending resistance and contact stress.

The study investigates addendum modification, known as profile shift, in gears. Increasing addendum thickness enhances bending resistance and reduces contact stress, while decreasing thickness increases bending stress. The profile shift coefficient quantifies this adjustment relative to the module. Factors chosen from KISSsoft's recommendations, depicted in Figures 1-3, play a crucial role in optimizing gear performance by influencing bending resistance and contact stress.

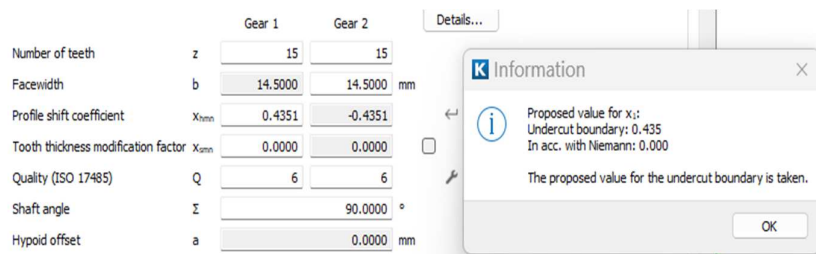


**Fig. 1.** Profile shift coefficient of 14.5°.

		Gear 1	Gear 2	
Number of teeth	z	15	15	
Facewidth	b	14.5000	14.5000	mm
Profile shift coefficient	$x_{hmn}$	0.0000	0.0000	← ↔
Tooth thickness modification factor	$x_{snn}$	0.0000	0.0000	<input type="checkbox"/>
Quality (ISO 17485)	Q	6	6	✂
Shaft angle	$\Sigma$		90.0000	°
Hypoid offset	a		0.0000	mm

Fig. 2. Profile shift coefficient of 20°.

		Gear 1	Gear 2	
Number of teeth	z	15	15	
Facewidth	b	14.5000	14.5000	mm
Profile shift coefficient	$x_{hmn}$	0.0000	0.0000	← ↔
Tooth thickness modification factor	$x_{snn}$	0.0000	0.0000	<input type="checkbox"/>
Quality (ISO 17485)	Q	6	6	✂
Shaft angle	$\Sigma$		90.0000	°
Hypoid offset	a		0.0000	mm

Fig. 3. Profile shift coefficient of 25°.

## 2.2 Results of Analysis

The following figure illustrates the gear pair generated through the design process. In this section, we explore the shared characteristics of gears characterized by three distinct pressure angles. The examination is centered on identifying and analyzing properties that are consistent across these gears, offering a comprehensive understanding of their design and performance aspects.



Fig. 4. Visual Representation of Gear System.

consistent regardless of the pressure angles, underscoring a feature that remains constant across different pressure angle arrangements.

Outer pitch diameter (mm)	[de]	70.898	70.898
Outer tip diameter (mm)	[dae]	77.582	77.582
Outer root diameter (mm)	[dfe]	62.543	62.543
Mean pitch diameter (mm)	[dm]	60.645	60.645
Mean tip diameter (mm)	[dam]	66.363	66.363
Mean root diameter (mm)	[dfm]	53.498	53.498
Inner pitch diameter (mm)	[di]	50.392	50.392
Inner tip diameter (mm)	[da]	55.143	55.143
Inner root diameter (mm)	[difi]	44.453	44.453

Fig. 5. Results of diameter.

### 2.2.1 Types of Diameter and Modules

The figures below (Figures 5–6) illustrate the gears' tip and pitch diameters, as well as their outer, mean, and inner diameters. Additionally, these dimensions are displayed in the technical drawing when the KISSsoft gear data is transferred to the SolidWorks application and transformed into a solid module. Interestingly, it is observed that these diameters remain

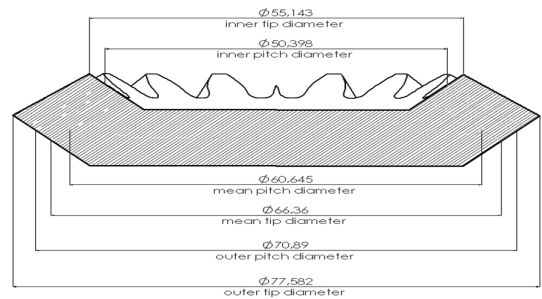


Fig. 6. Types of diameter.

Figure 7 clearly presents the inner, main, and outer modules. Particularly, the modulus is distinctly illustrated as the pitch diameter divided by the number of teeth. This fundamental relationship between modulus and geometry provides a crucial insight into the structural characteristics of the gears being examined. Understanding this relationship is essential for comprehending the fundamental

design aspects and performance attributes of the gears in the depicted configuration.

Outer normal module (mm)	[men]	4.7265	
Transverse module, outside (mm)	[met]	4.7265	4.7265
Mean normal module (mm)	[mmn]	4.0430	
Mean transverse module (mm)	[mmt]	4.0430	4.0430
Inner normal module (mm)	[min]	3.3595	
Transverse module, inside (mm)	[mit]	3.3595	3.3595

Fig. 7. Types of modules.

### 2.2.2 Examining Cone Distances

The cone distance is vital for mounting bevel gears, defining the linear separation between reference points at the intersections of reference diameters. Mean cone distance measures from the pitch cone's apex to the center of the face width, while inner cone distance denotes the gap between the inner teeth ends and the pitch cone's apex. Figure 8 visually demonstrates these cone distances, aiding comprehension of crucial dimensions for the geometry and mounting of bevel gears.

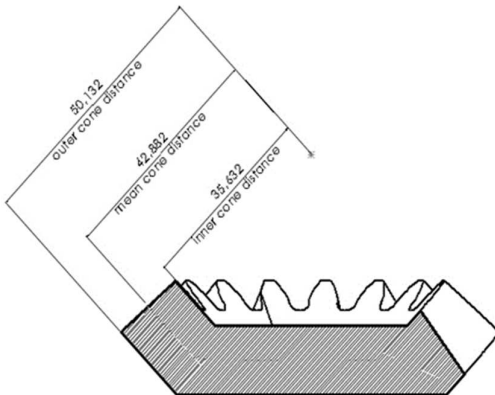


Fig. 8. Cone Distances.

### 2.2.3 Analysis of Specific Sliding Characteristics

Sliding velocity depicts precise tooth contact movement in mating gears. Figure 9 shows the sliding graph for a 14.5-degree pressure angle gear, revealing contact timing and extent. The first gear's contact starts below  $|3|$  and extends beyond it, while the second gear's contact starts beyond  $|3|$  and ends within it. Contact initiation occurs at 12 degrees, concluding at 6 degrees. This graph offers insights into gear interaction dynamics.

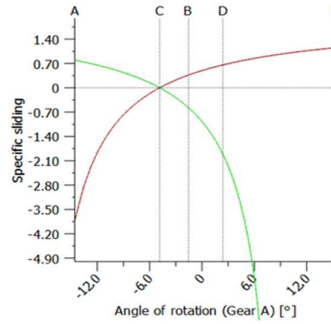


Fig. 9. Specific sliding graph of 14.5° [14].

In Fig. 10, the sliding graph for a gear with a 20-degree pressure angle is depicted. The red line corresponds to the first gear, and the green line represents the second gear. Key points on the graph are labeled accordingly:

- Point A: Marks the initiation of gear contact.
- Point B: Signifies the transition from contact with two teeth to one tooth.
- Point C: Represents the contact point where the division circles intersect.
- Point D: Denotes the transition from contact with one tooth back to two teeth.
- Point E: Marks the completion of gear contact.

Upon observation, we note the first gear's contact starts below  $|3|$  and ends beyond  $|3|$ , while for the second gear, contact begins below  $|3|$  and ends above  $|3|$ . Specifically, contact starts at 12 degrees and ends at 6 degrees. This sliding graph visually illustrates the dynamic gear interaction, revealing contact and disengagement phases during meshing.

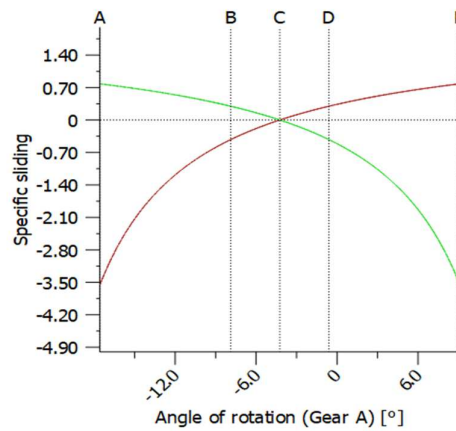


Fig. 10. Specific sliding graph of 20° [14].

In Fig. 11, the sliding graph depicts the gear with a 25-degree pressure angle. Both gears display contact start and end values below  $|3|$ .

Notably, contact initiation began at 16 degrees and concluded at 4 degrees. This graphical representation offers valuable insights into the sliding behavior of the gears, highlighting that the entire phase of gear contact occurs below the threshold of |3|. The visual depiction of these specific sliding characteristics enhances our understanding of the dynamics of gear interaction, particularly in terms of contact initiation, progression, and conclusion for the specified pressure angle.

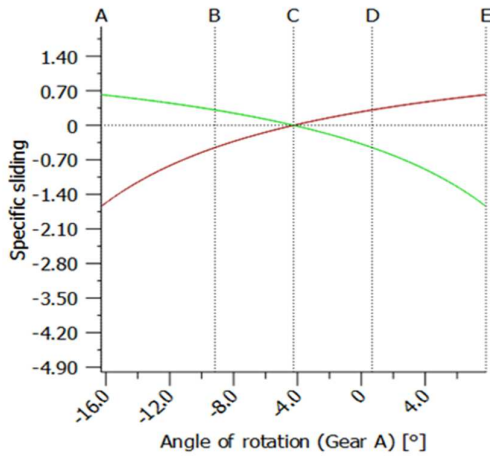


Fig. 11. Specific sliding graph of 25° [14].

**2.2.5 Understanding Gear Loss Factor HV**

The gear loss factor HV, derived from gear geometry, is pivotal in power loss calculations. It integrates sliding speed, coefficient of friction, and load across the contact path. Assessing HV is critical because gearbox power loss, under nominal loads, is predominantly influenced by gear losses. Ohlendorf introduced a load-dependent method [15] for predicting losses on spur gears, enabling computation of power loss at gear tooth contact using Equation (1).

$$P_{VZP} = P_{IN} \times H_V \times \mu_m \quad (1)$$

Equation (1), utilizing P\_IN for gearbox power and μ\_m for the coefficient of friction, determines gear loss as detailed in Table 4. The table demonstrates an increase in mesh efficiency with higher pressure angles, emphasizing the pivotal role of gear geometry in enhancing mesh performance.

Table 4

Gear loss and mesh efficiency			
Results/Degrees	14.5°	20°	25°
Loss factor (HV)	0.194	0.171	0.174
Gear power loss (kW)	0.178	0.147	0.123
Meshing efficiency (%)	97.627	98.036	98.355
Coefficient of friction μm	0.123	0.115	0.103

**2.2.6 Analysis of Active Forces in Gear Meshing**

The analysis considers active forces on gears at two mesh locations, with the pinion driving. At contact, Fn1 opposes the pinion flank, and Fr1 is generated tangentially due to sliding velocity. Equivalent forces Fr2 and Fn2 act oppositely. Figure 12 visually depicts these forces' orientations and relationships within the gear meshing context.

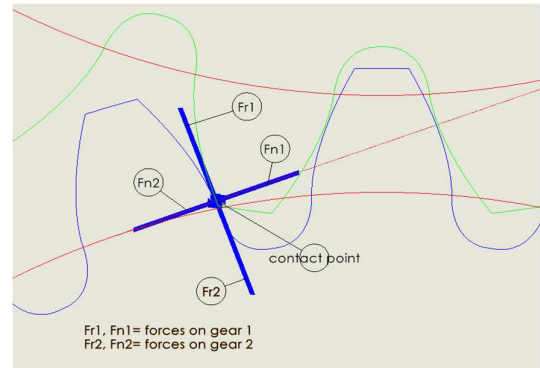


Fig. 12. - Shows radial forces and normal forces calculated by KISSsoft [14].

Table 5

Forces		
Pressure Angle/Forces	Radial Force	Normal Force
14.5°	799.9	4517.9
20°	1225.7	4654.7
25°	1442.2	4826.1

The modeling and KISSsoft calculations reveal several key findings. Firstly, power loss in the sprocket decreases with increasing pressure angle, while mesh elongation increases. Secondly, specific sliding graphs for three pressure angles, including the optimal 25° angle, were computed for gears optimized for a

gearbox with 7.5 kW input power and 540 1/min speed. Thirdly, variations in pressure angle impact gear macrogeometry values such as cone distance, outer modulus, mean modulus, inner modulus, outer diameter, mean diameter, and inner diameter.

Analysis of specific sliding graphs indicates that the gear pair achieving a value of  $|3|$  for both gears simultaneously has a pressure angle of  $25^\circ$ . Additionally, a gear pair with a  $14.5^\circ$  pressure angle requires an undercut boundary of 0.435. These findings emphasize that the minimum number of teeth increases as pressure angle decreases, providing insights into design considerations and trade-offs associated with different pressure angles in gear systems.

### 3. RESULTS

In a detailed analysis, a gear pair with 15 teeth and pressure angles of  $14.5^\circ$ ,  $20^\circ$ , and  $25^\circ$  was examined using advanced computational tools. Through modeling and calculations with KISSsoft and SolidWorks, the study explored gear performance nuances across different pressure angles.

The insights assembled from this study are multi-layered:

1. Power Loss and Mesh Elongation: It was observed that the power loss in the sprocket decreases as the pressure angle decreases, which suggests a more efficient power transmission system. However, this decrease in power loss is accompanied by an increase in mesh elongation, highlighting a trade-off between efficiency and structural integrity.
2. Optimal Pressure Angle: Specific sliding graphs revealed that gears with a pressure angle of  $25^\circ$  exhibit optimal performance for the gearbox operating at 7.5 kW input power and 540 1/min speed. This finding underscores the importance of selecting the appropriate pressure angle to maximize gear efficiency and longevity in specific operational contexts.
3. Impact on Gear Macrogeometry: Changes in the pressure angle significantly influenced various values related to gear macrogeometry, including cone distance, modulus, and diameter parameters. Understanding these effects is crucial for

fine-tuning gear designs to meet performance requirements and operational constraints.

These findings not only enhance our understanding of gear behavior under different pressure angles but also offer practical insights for optimizing gear design and performance in real-world applications. Moving forward, future research directions aim to explore deeper surface roughness measurements, explore advanced techniques for surface characterization, and develop predictive models to further refine gear design and enhance operational reliability. By continually advancing our knowledge and methodologies in gear analysis and design, we can drive innovation and efficiency in mechanical systems across various industries.

### 4. REFERENCES

- [1] Can, E. (2019). Optimization of gear geometrical parameters [Master's thesis]. Yıldız Technical University.
- [2] Gou, X., Li, G., & Zhu, L. (2022). Dynamic characteristics of a straight bevel gear drive system considering multi-state meshing and time-varying parameters. *Mechanism and Machine Theory*, 171, 1–7. <https://doi.org/10.1016/j.mechmachtheory.2022.104779>.
- [3] Menküç, R., Uysal, L. K., & Topgül, T. (2002). Effect of profile modification on noise in involute gear pair. *International Journal of Automotive Science and Technology*, 5(2), 79–84. <https://doi.org/10.30939/ijastech..881879>.
- [4] Miller, R. (2017). Designing very strong gear teeth by means of high pressure angles. *Gear Technology*, 34(4), 66–79.
- [5] Ramamurti, A., Sujatha, C., & Vijayandre, H. (1996). Static and dynamic analysis of spur and bevel gears using fem. *Mechanism and Machine Theory*, 33(8), 1177–1993. [https://doi.org/10.1016/S0094-114X\(97\)00112-2](https://doi.org/10.1016/S0094-114X(97)00112-2).
- [6] Unal, E., & Taşdemir, V. (2018). Investigation of effect on the contact stress of gear rotational speed in helical gears. *Journal*



- of Engineering Sciences and Design, 383–389.
- [7] Chen, W., Chen, S., Hu, S., Tang, J., & Li, H. (2020). Dynamic analysis of a bevel gear system equipped with finite length squeeze film dampers for passive vibration control. *Mechanism And Machine Theory*, 147, 1–18. <https://doi.org/10.1016/j.mechmachtheory.2019.103779>.
- [8] Zhang, F., Tian, X., & Cui, H. (2012). The modification design of involute straight bevel gear. *IERI Procedia*, 3, 52–59. <https://doi.org/10.1016/j.ieri.2012.09.010>.
- [9] Fuentes, A., Iserte, J., Gonzales-Perez, I., & Sanchez-Marin, F. (2011). Computerized design of advanced straight and skew bevel gears produced by precision forging. *Computer Methods in Applied Mechanics and Engineering*, 200(29–32), 2363–2377. <https://doi.org/10.1016/j.cma.2011.04.006>.
- [10] Litvin, F., Fuentes, A., Fan, Q., & Handschuh, R. (2002). Computerized design, simulation of meshing, and contact and stress analysis of face-milled formate generated spiral bevel gears. *Mechanism and Machine Theory*, 37(5), 441–459. [https://doi.org/10.1016/S0094-114X\(01\)00086-6](https://doi.org/10.1016/S0094-114X(01)00086-6).
- [11] Schuman, S., Senf, M., & Schlecht, B. (2014). Increasing the load-capacity of bevel gears by the use of modern optimization methods. 180–189. <https://doi.org/10.1533/9781782421955.180> <https://doi.org/10.21923/jesd.371240>.
- [12] Litvin, F., Kuan, C., Kieffer, J., Bossler, R., & Handschuh, R. (1990). Straddle design of spiral bevel and hypoid pinions and gears. National Aeronautics and Space Administration. <https://ntrs.nasa.gov/api/citations/19910005289/downloads/19910005289.pdf>.
- [13] Errichello, R. (2013). Gear contact temperature and scuffing risk analysis. In *Encyclopedia of Tribology* (pp. 1466–1470). Springer.
- [14] Mutlu, Y.M. (2023). Comparison of bevel gears with different pressure angle and sound analysis. Unpublished M.Sc. Thesis, 2023-M.Sc.-095, Aydin Adnan Menderes University, Turkey.
- [15] Ohlendorf, H. (1958). Verlustleistung und erwärmung von stirnrädern [Doctoral Thesis]. Technische Hochschule München.
- [16] Demircioglu, P. (2017). Topological Evaluation of Surfaces in Relation to Surface Finish, *Comprehensive Materials Finishing*, 3, 17, pp. 243-260.
- [17] Bogrekci, I., Demircioglu, P. (2017). Evaluation of Surface Finish Quality Using Computer Vision Techniques, *Comprehensive Materials Finishing*, 3, 18, pp. 261-275.

### Comparația angrenajelor conice cu unghi de presiune diferit

**Rezumat:** La roțile dințate, ambreiajul începe în punctul în care suprafața laterală a limbii rotative atinge partea superioară a dintelui angrenajului rotit și se termină în punctul în care partea superioară a dintelui angrenajului rotativ atinge suprafața laterală a angrenajului rotit. Pe măsură ce unghiul de presiune scade, raportul ambreiajului crește, dar numărul minim de dinți este cel mai mare. În acest studiu, 3 perechi de angrenaje cu unghiuri de presiune de

14,5°, 20° și 25° au fost proiectate folosind KISSsoft pentru un distribuitor de îngrășăminte cu putere de intrare de 7,5 KW și viteză de intrare de 540 1/min. În urma studiului, s-a ajuns la concluzia că cel mai eficient angrenaj pentru această cutie de viteze a fost angrenajul cu un unghi de presiune de 25°.

**Pınar DEMIRCI OGLU**, Prof. Dr. techn., Aydin Adnan Menderes University (ADU), Mechanical Engineering Department, pinar.demircioglu@adu.edu.tr, 09010 Aydin, TURKEY; Visiting Professor, Technical University of Munich (TUM), Mechanical Engineering, ge74hez@mytum.de, 85748 Garching, GERMANY

**Ismail BOGREKCI**, Professor, Aydin Adnan Menderes University (ADU), Mechanical Engineering Department, ibogrekci@adu.edu.tr, 09010 Aydin, TURKEY.

**Yegane Mediha MUTLU**, Master Student, Aydin Adnan Menderes University, Mechanical Engineering, yegane1996.ym@gmail.com, Aydin, TURKEY; R&D Engineer, Türkay Tarım Makinaları, mediha.mutlu@turkay.com.tr, Izmir TURKEY.